Supporting Information

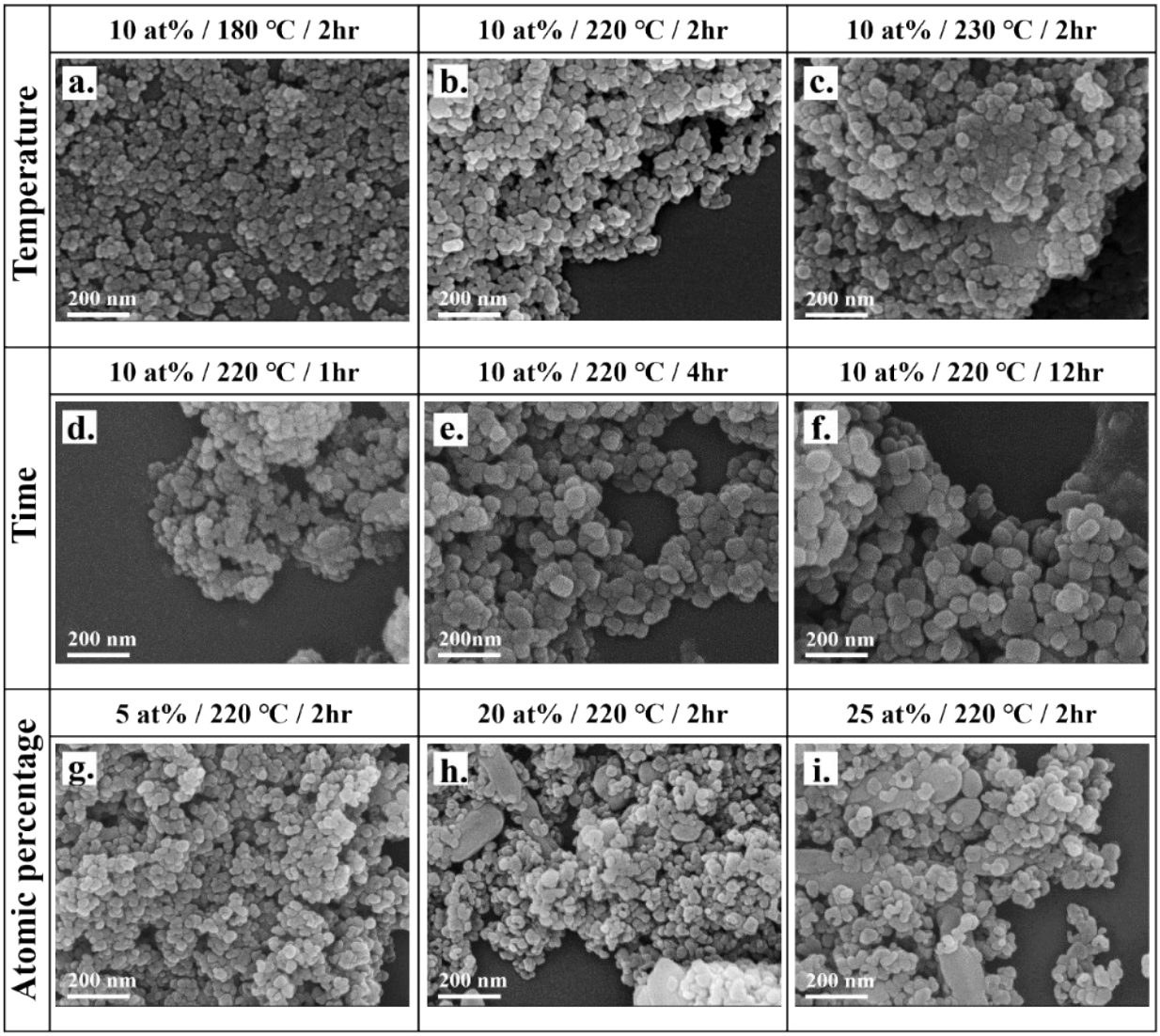

Fig. S1 FE-SEM images of doped $BaTiO_3$ hollow structures synthesized at (a–c) 10 at% for 2 h at (a) 180, (b) 220, and (c) 230 °C; (d–f) 10 at% at 220 °C for (d) 1, (e) 4 h, and (f) 12 h; and (g–i) 220 °C for 2 h at (g) 5, (h) 20, and (i) 25 at%.

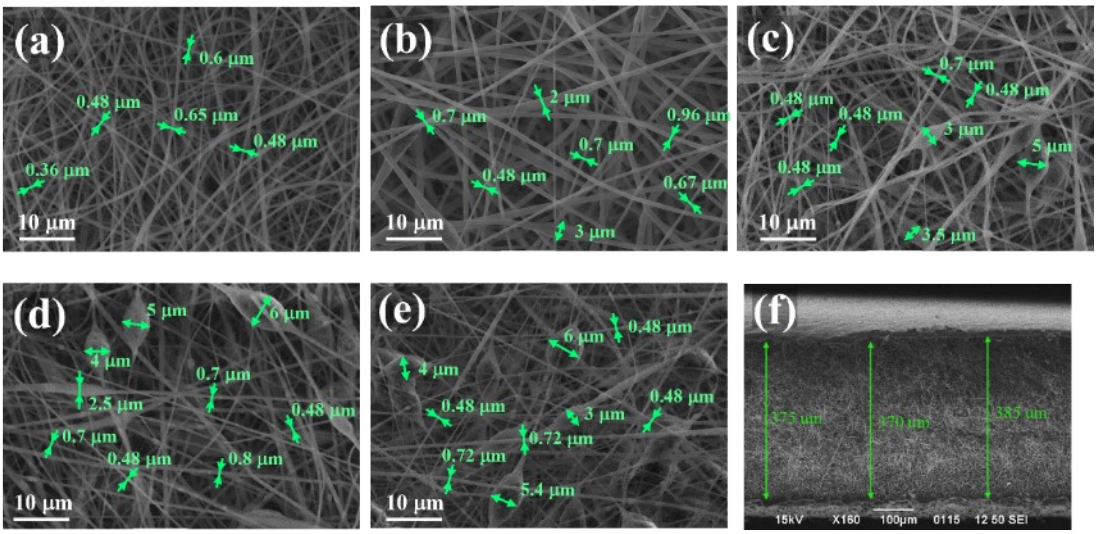

Fig. S2 (a–e) SEM images of (a) 0, (b) 1, (c) 5, (d) 10, and (e) 15 wt% Eu_2O_3-$BaTiO_3$/PVDF-HFP nanofibers. (f) SEM cross-section of 10 wt% Eu_2O_3-$BaTiO_3$/PVDF-HFP nanofibers.

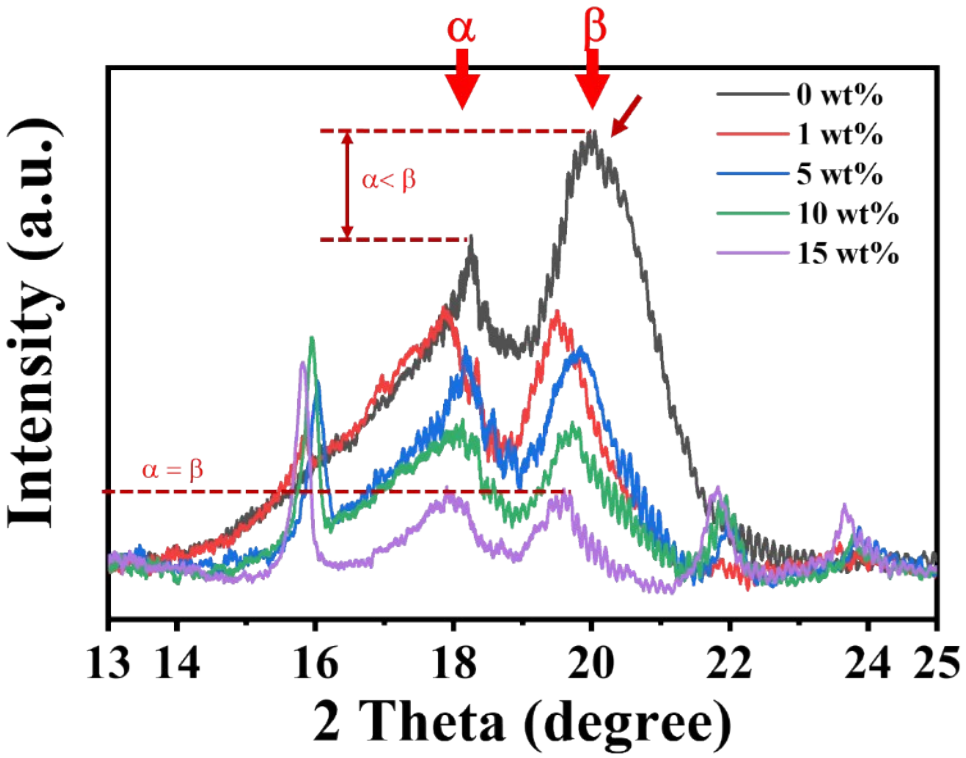

Fig. S3 The XRD patterns of PVDF α and β phase with different weight percentages of Eu_2O_3-$BaTiO_3$/PVDF-HFP

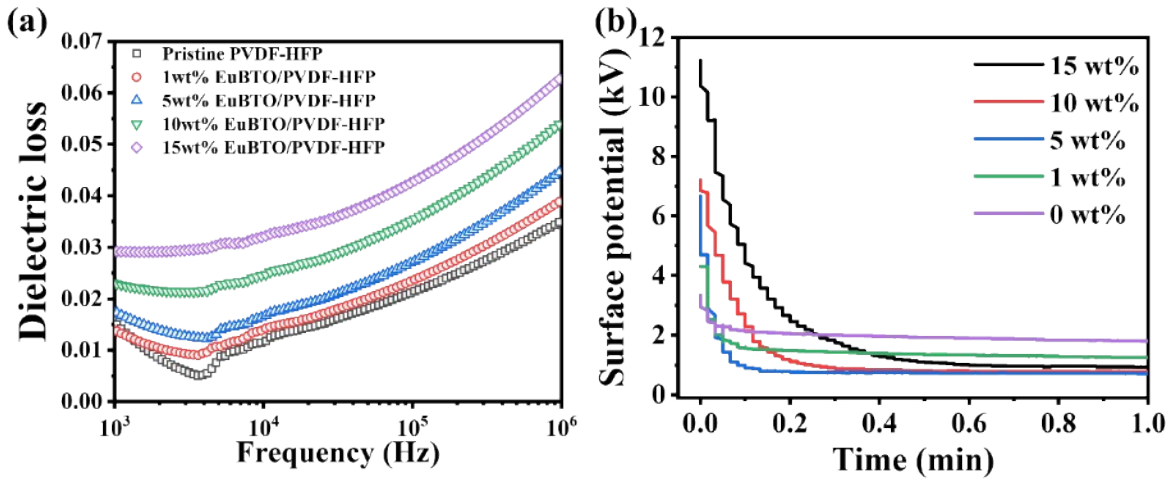

Fig. S4 (a) Dielectric loss of various-weight-percentage Eu_2O_3-$BaTiO_3$/PVDF-HFP nanofiber mats plotted with respect to frequency. (b) retention times of the surface potential for different percentages of Eu_2O_3-doped $BaTiO_3$/PVDF-HFP composite after contact friction with the Kapton film.

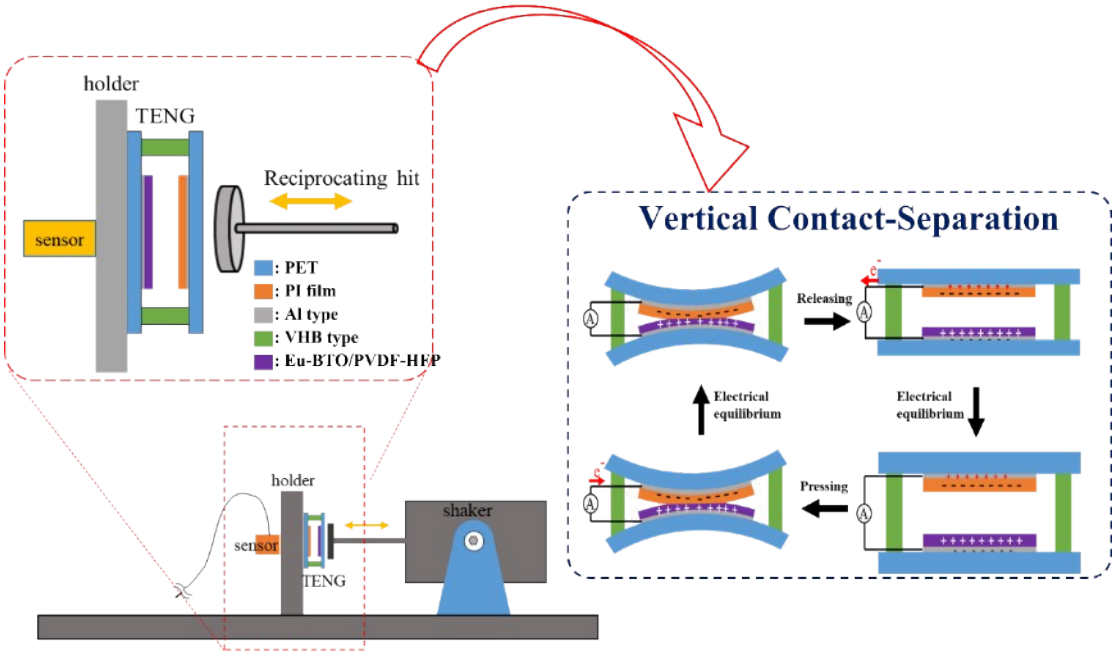

Fig. S5 Schematic representation of the working mechanism of the electrospun Eu_2O_3-$BaTiO_3$/PVDF-HFP electrospun-nanofiber TENG (device size: 1 cm × 1 cm).

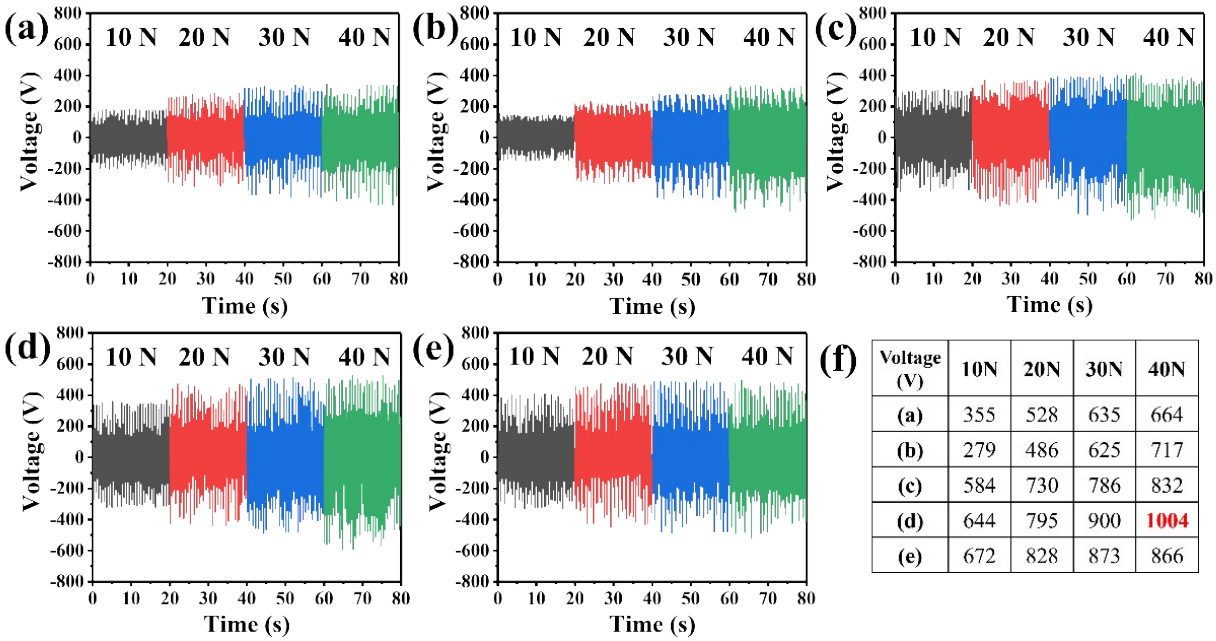

(f)

Voltage (V)	10N	20N	30N	40N
(a)	355	528	635	664
(b)	279	486	625	717
(c)	584	730	786	832
(d)	644	795	900	**1004**
(e)	672	828	873	866

Fig. S6 (a–e) Electrical output voltages of (a) 0, (b) 1, (c) 5, (d) 10, and (e) 15 wt% Eu_2O_3-$BaTiO_3$/PVDF-HFP nanofibers, measured at various mechanical forces. (f) summarized the electrical output voltage of various weight percentage of Eu_2O_3-$BaTiO_3$/PVDF-HFP nanofibers, measured at various mechanical forces.

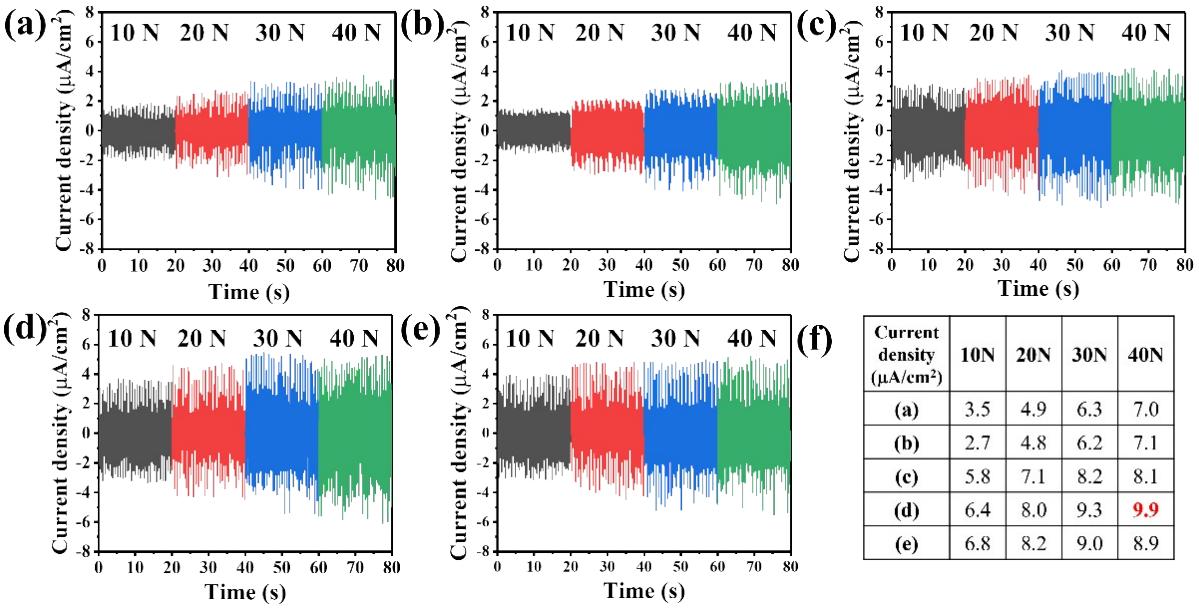

(f)

Current density (μA/cm²)	10N	20N	30N	40N
(a)	3.5	4.9	6.3	7.0
(b)	2.7	4.8	6.2	7.1
(c)	5.8	7.1	8.2	8.1
(d)	6.4	8.0	9.3	**9.9**
(e)	6.8	8.2	9.0	8.9

Fig. S7 (a–e) Electrical output current densities of (a) 0, (b) 1, (c) 5, (d) 10, and (e) 15 wt% Eu_2O_3-$BaTiO_3$/PVDF-HFP nanofibers, measured at various mechanical forces. (f) summarized the electrical output current density of various weight percentage of Eu_2O_3-$BaTiO_3$/PVDF-HFP nanofibers, measured at various mechanical forces.

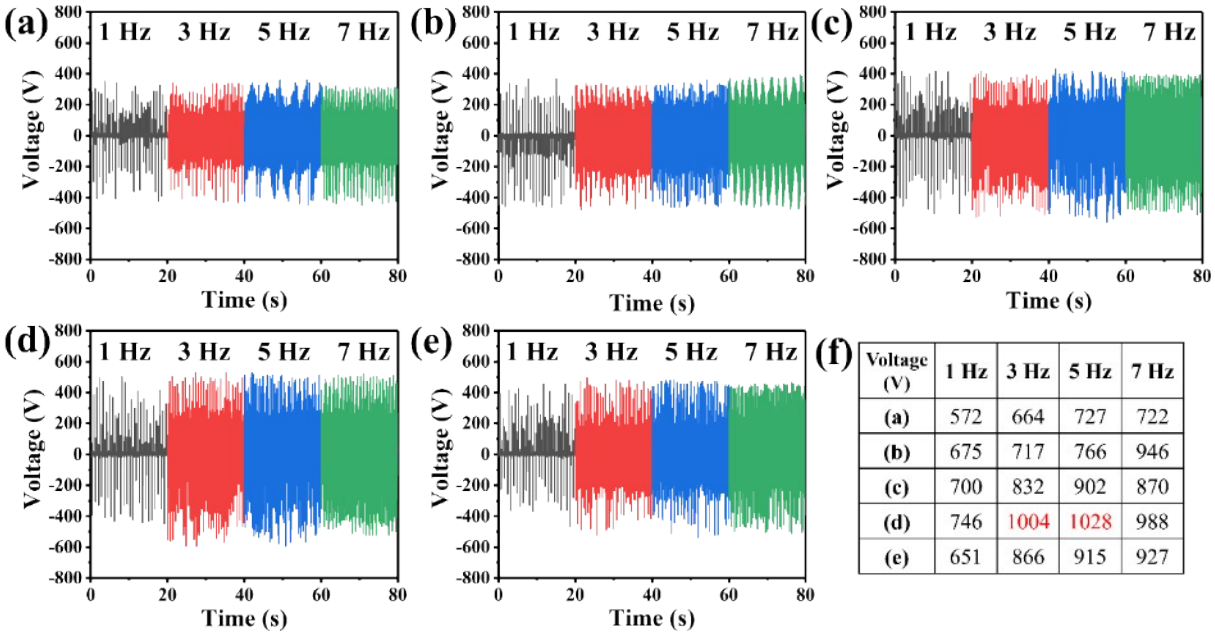

(f)

Voltage (V)	1 Hz	3 Hz	5 Hz	7 Hz
(a)	572	664	727	722
(b)	675	717	766	946
(c)	700	832	902	870
(d)	746	1004	1028	988
(e)	651	866	915	927

Fig. S8 (a–e) Electrical output voltages of (a) 0, (b) 1, (c) 5, (d) 10, and (e) 15 wt% Eu_2O_3-$BaTiO_3$/PVDF-HFP nanofibers, measured at various frequencies. (f) summarized the electrical output voltage of various weight percentage of Eu_2O_3-$BaTiO_3$/PVDF-HFP nanofibers, measured at various frequencies.

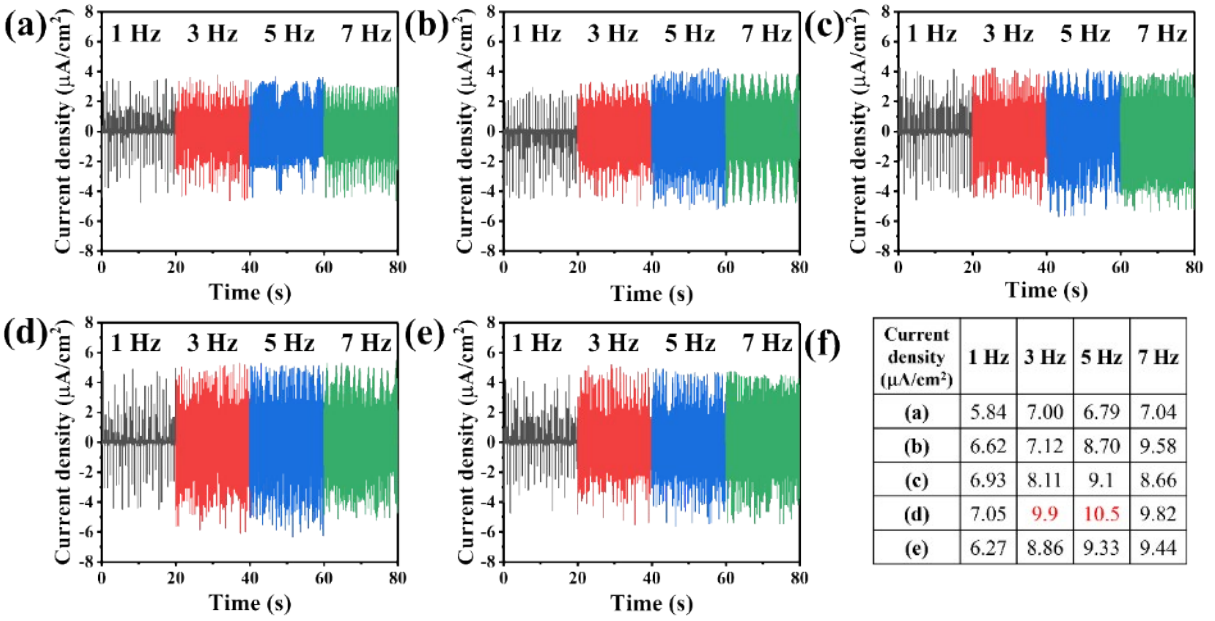

(f)

Current density (μA/cm²)	1 Hz	3 Hz	5 Hz	7 Hz
(a)	5.84	7.00	6.79	7.04
(b)	6.62	7.12	8.70	9.58
(c)	6.93	8.11	9.1	8.66
(d)	7.05	9.9	10.5	9.82
(e)	6.27	8.86	9.33	9.44

Fig. S9 Electrical output current densities of (a) 0, (b) 1, (c) 5, (d) 10, and (e) 15 wt% Eu_2O_3-$BaTiO_3$/PVDF-HFP nanofibers, measured at various frequencies. (f) summarized the electrical output current densities of various weight percentage of Eu_2O_3-$BaTiO_3$/PVDF-HFP nanofibers, measured at various frequencies.

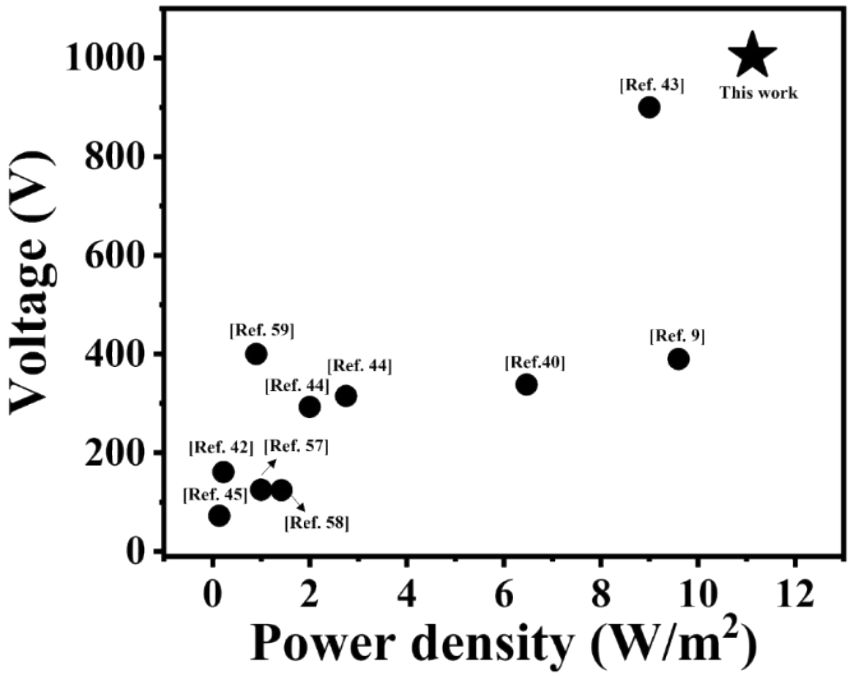

Fig. S10 Open-circuit voltages and peak power densities of TENGs reported herein and previously in the literature (Table 1).

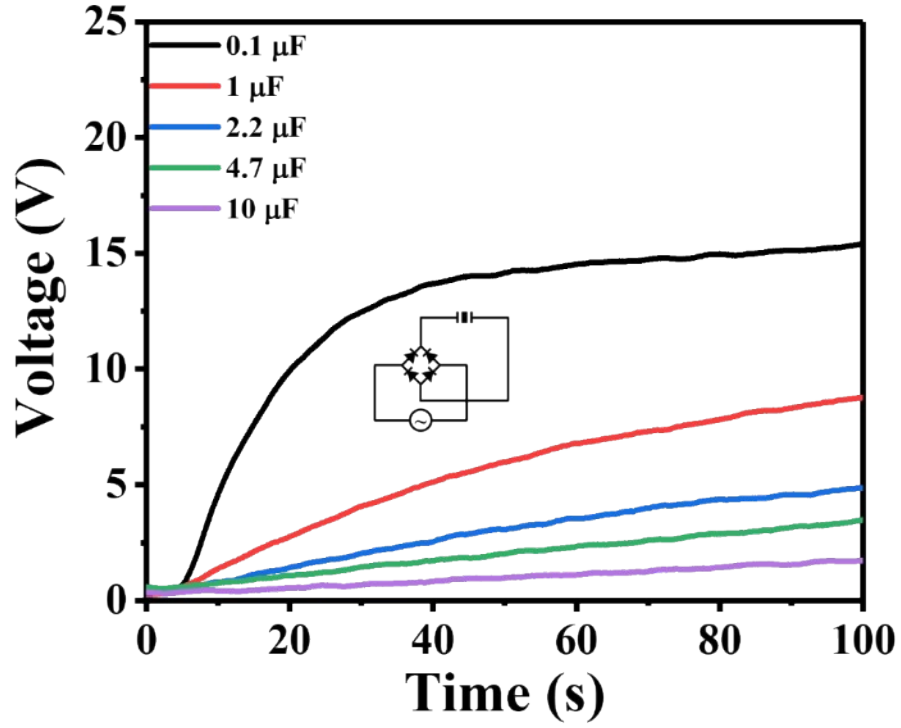

Fig. S11 Charging capacitors of various capacitances with pristine PVDF-HFP electrospun-nanofiber TENGs.